International Journal of Mechanical and Production Engineering Research and Development (IJMPERD)
ISSN (P): 2249–6890; ISSN (E): 2249–8001
Vol. 9, Issue 6, Dec 2019, 451–462

Original Article

EFFECT OF KNUDSEN NUMBER ON BLUNT BODY DURING HYPERSONIC SPEEDS FOR REDUCING DRAG

MAMIDI AJAY SAGAR[1], SYED MUNVAR ALI[2], A. NAVYA MANJARI[3] & L. SUSHMA[4]

[1]*Assistant Professor, Department of Aeronautics, School of Aeronautics, Neemrana, Rajasthan, India*

[2]*CFD Engineer, DRDL, Hyderabad, Andhra Pradesh, India*

[3]*M. Tech Student, Department of Aerospace Engineering, JNTUH, Andhra Pradesh, India*

[4]*Associate Professor, MRCET, Department of Aeronautical Engineering, Andhra Pradesh, India*

ABSTRACT

This paper employs the Navier-Stokes equations, which are modified to include a rotational non- equilibrium relaxation model to analyse the heat transfer, drag, and shock stand of distance for hypersonic flow past an axisymmetric blunt body for various levels of rarefaction including the rotational non-equilibrium effect. The commercial flow solver FLUENT is used to calculate the numerical solutions for laminar viscous hypersonic flow past a blunt body at Knudsen number (K_n) in continuum-transition regime with and without rotational non-equilibrium. The effects of rarefaction in the continuum-transition regime are modelled by applying the Maxwell velocity slip and temperature jump boundary conditions on the surface. The effects of the rotational non-equilibrium terms are discussed in this paper for both the continuum $K_n \cong 0.1$ and no slip flow regime $K_n \leq 0.1$. Study is performed for (M_∞= 6.5, 7, 7.1 and 8). Finally we conclude by comparing drag and heat transfer changes by changing K_n number. Effect of increase in Mach number is also studied and concluded.

KEYWORDS: Knudsen Number, Blunt Body, Flow Regime, Hypersonic Speeds & Rarefaction Effects

Received: Jul 26, 2019; **Accepted**: Aug 17, 2019; **Published**: Nov 04, 2019; **Paper Id**.: IJMPERDDEC201939

1. INTRODUCTION

During the first stage of atmospheric re-entry, vehicles undergo high heat loads and increased drag due to the high velocity and temperature. At these altitudes, the flow can no longer be considered to be in the continuum regime due to the effect of reduced atmospheric density, referred to as rarefaction. Many commercial flow solvers are not able to accurately predict these flows outside the continuum regime, which challenges the design and optimization of space vehicle geometries under those conditions. Simulating these flow conditions is difficult; however, creating a flow solver capable of accurately predicting these flows are much more cost effective compared to wind tunnel testing in an actual hypersonic environment.

Rarefaction is characterized by the Knudsen number, a non-dimensional parameter given by:

$$K_n = \frac{\lambda}{L} \tag{1}$$

Where $K_n$the Knudsen number isλ is mean free path of the molecules in free stream and L is the characteristic length.

The flow is considered to be within continuum regime when Knudsen number is very small <0.002. An accurate solution can be calculated in continuum regime using Navier-Stokes equation without slip conditions. These equations break down as rarefaction effect increase. It is possible to modify NS equations in order to obtain accurate results in the continuum-transition slip regime. This is defined as $0.002<K_n<0.1$. This is done by implementing Maxwell Slip wall boundary conditions. Another significant effect that needs to be considered when hypersonic vehicles re-enter is the atmosphere effect of a rotational non-equilibrium.

In this study, ANSYS Fluent flow solver is used to implement the Maxwell a slip boundary conditions as well as the rotational thermal non-equilibrium for the calculation of rare flow fields. The effects of a two-temperature thermal non-equilibrium model are analysed for blunt leading edge geometry. An axisymmetric blunt body at various Knudsen numbers. The geometry is then optimized for the reduction of heat transfer and drag at a chosen Knudsen number with the temperature model.

2. BACKGROUND

Hypersonic flows have the properties of Shock stand-off distance, Real gas, entropy change, Low density, thermal non-equilibrium and molecular dissociation. The density of gas behind shock wave increases as Mach number increases. This causes the shock wave stand-off distance to decrease with Mach number. This decreased shock stand-off distance mixes with high temperature due to kinetic energy causes internal energy. This heat transfer can be reduced by reducing the leading edge radius and the drag on the body also increases. We can reduce both drag and heat transfer with the optimization of the body.

The high temperature associated with hypersonic flows can also increase thermal non equilibrium in rotational and vibration modes. For a diatomic gas such as nitrogen, the vibration mode activates at 3300K and become significant above 5000K temperature.

The 3D navier stokes equation for a diatomic gas in conservation law form in Cartesian coordinates. They can be written as

$$\frac{\partial Q}{\partial t}+\frac{\partial E}{\partial x}+\frac{\partial F}{\partial y}+\frac{\partial G}{\partial x}+\frac{\partial E_v}{\partial x}+\frac{\partial F_v}{\partial y}+\frac{\partial G_v}{\partial z}=S \tag{2}$$

The stress tensor, τ_{ij} and heat flux vector q_{ij} are obtained from Chapman-Enskog expansion.

$$\tau_{ij}=\tau_{ij}^0+\tau_{ij}^1+\tau_{ij}^2+\cdots+\tau_{ij}^k+O(K_n^{n+1}) \tag{3}$$

$$q_{ij}=q_{ij}^0+q_{ij}^1+q_{ij}^2+\cdots+q_{ij}^n+O(K_n^{n+1}) \tag{4}$$

The navier stokes equations are obtained by taking first two terms of expansion, second order terms, in this stress tensor and heat flux vector expansion becomes

$$\tau_{ij}=\tau_{ij}^0+\tau_{ij}^1=-\frac{2\mu\overline{\partial u_i}}{\partial x_i} \tag{5}$$

$$q_{ij}=q_{ij}^0+q_{ij}^1=-\frac{k\partial T}{\partial x_i} \tag{6}$$

The local viscosity of the flow is calculated using Sutherland's law

$$\mu = \mu_{ref}\left(\frac{T}{T_{ref}}\right)^{\frac{3}{2}}\frac{(T_{ref}+S)}{T+S} \tag{7}$$

Where μ_{ref} and T_{ref} are the reference viscosity and temperature; S is the Sutherland temperature of the gas; and T is the local temperature. In order to close the system of equations an equation of state is used, in this case, the ideal-gas law.

3. RAREFACTION EFFECTS

As space vehicles travel through the atmosphere and into the lower earth orbit, the density of the atmosphere decreases. This reduced density is called the rarefaction. The degree of rarefaction is characterized by the Knudsen number:

$$K_n = \frac{\lambda}{L} \tag{8}$$

Where K_n the Knudsen number is λ is mean free path of the molecules in free stream and L is the characteristic length.

The mean free path is the average distance travelled by a particle in the flow between collisions. In general, the mean free path of a molecule is given by Equation

$$\lambda = \frac{RT}{\sqrt{2}\pi d^2 N_A P} \tag{9}$$

Where R is the universal gas constant, T is the free stream temperature, d is the average molecule diameter, NA is Avogadro's number and P is the free stream pressure.

In the case of standard air, Equation 9 can be simplified to Equation 10.

$$\lambda = \frac{\mu}{\rho}\sqrt{\left(\frac{\pi}{2RT}\right)} \tag{10}$$

Where ρ is the free stream density and μ is the viscosity.

It can be seen in Equation-10 that as the free stream density decreases, the mean free path increases and thus increasing the effect of rarefaction. At extremely flow Knudsen numbers (Kn≤ 0.01), the flow is in the continuum regime. Some equations used to model flow, such as the Euler and Navier-Stokes equations, are valid only in the continuum regime. As the Knudsen number increases, flow becomes rare field and enters the continuum-transition regime (Kn ≤10) and the Navier-Stokes equations are no longer able to accurately predict the flow. The validity of Navier-Stokes equations can be extended to Kn ≤ 0.1 by using Maxwell's slip flow boundary conditions [5] on the wall. The mathematical equations valid for each flow regime are shown in figure 1.1.

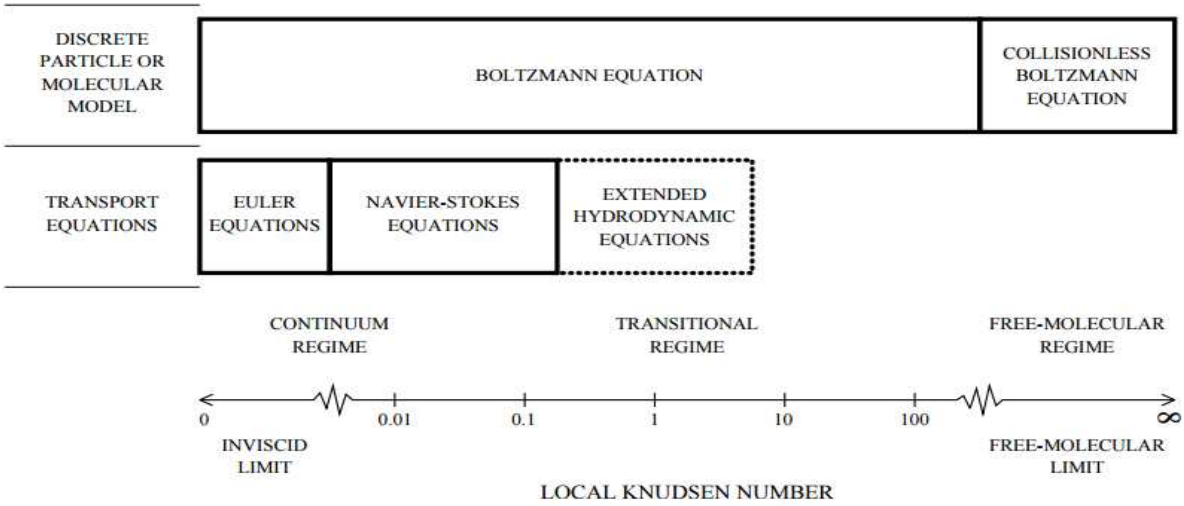

Figure 1: Flow Regimes and Appropriate Equations for Modelling the Flow at a Given Knudsen Number.

4. DESIGN AND MODELLING

In this chapter, the axisymmetric blunt body simulations in hypersonic flow are performed for four Knudsen numbers (0.002, 0.01, 0.05 and 0.1) at (M_∞= 6.5, 7.1, 7.5 & 8). The Maxwell's slip boundary conditions for slip velocity and temperature jump at the wall are employed in the simulations. The maximum heat transfer and the drag coefficients are obtained for each simulation. The geometry and free stream flow conditions used in the simulations correspond to the Lobby's ballistic range experiments and are as given in Ref. [5].

The leading edge radius of the sphere is 6.35 mm. Since the body shape is axisymmetric, only a quarter of the sphere is used for simulation of the flow. The quarter geometry of the sphere used is shown in figure 2. In the simulations, a cylindrical body shape is attached to the rear face of the sphere also shown in figure 2 to exclude the wake effects. A structured mesh around the geometry along with a cylindrical body attached is generated using ICEM-CFD. A slice of the final mesh is shown in figure 2. A mesh was chosen based on an extensive mesh validation study conducted by Seager [3], who employed several types of meshes of varying densities shown in figure 3 and concluded that the segmented mesh (35–105–10)x400 was the most efficient mesh with acceptable accuracy.

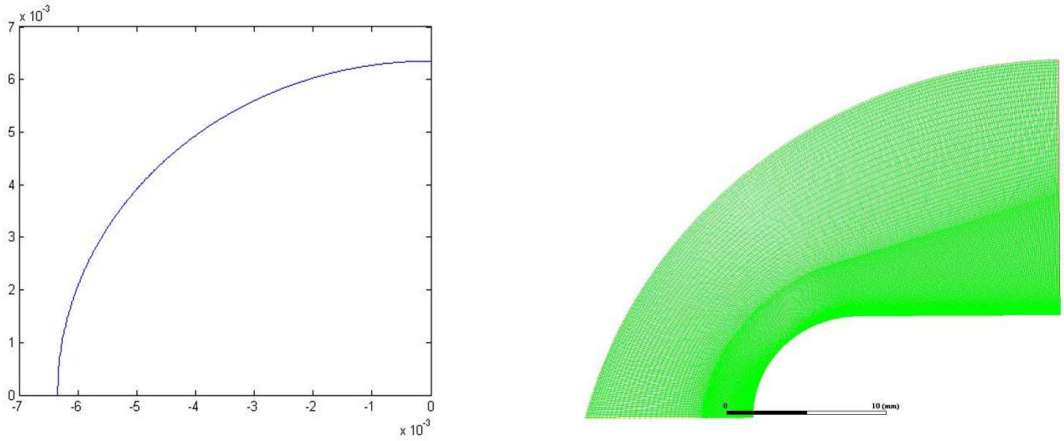

Figure 2: Axis Symmetric Blunt Geometry and Mesh.

		-------- Sphere --------		-------- Random Body Shape--------		
Mesh Type	*Mesh Size*	*C_D error*	*HT error*	*C_D error*	*HT error*	*Max y+*
Reference	**631x1250**	----------	----------	----------	----------	**0.87**
Uniform	80x200	0.1	29.3	7.3	26.5	3.64
	120x200	0.1	18.6	5.5	18.9	2.88
	160x400	0.1	9.3	3.4	11	2.27
	200x400	0	8.8	2.8	10.6	2.14
Segmented	(390-10)x400	0	4.0	0.7	2.6	.99
	(85-115)x400	0	8.3	1.5	6.5	.85
	(44-146-10)x400	0	7.3	1.7	5.8	.85
	(25-75-10)x400	0	8.3	2.7	11.7	1.00
Mesh of Choice	**(35-105-10)x400**	**0**	**7.5**	**2.2**	**5.8**	**0.76**

Figure 3: Validation Study Conducted.

5. NUMERICAL STUDY

Second order implicit algorithm used for spatial accuracy and dual time stepping transient flow field with multi-grid convergence acceleration is employed and the transient flow field is converged at every global time step. The fluid is treated as compressible perfect gas with composition of standard air. The $k-\varepsilon$ shear-stress transport (SST) model is used for turbulence modelling. The body surfaces of the inlet are assumed to be no-slip and adiabatic. The free stream flow conditions are obtained from Lobby's experiment and are given in Ref. [5]. The free stream Mach numbers are 6.5, 7.1, 7.5 and 8; the temperature is 293K; the air species distribution is 23.3 percent O_2 and 76.7 percent N_2. The wall is kept at a constant temperature of 1000 K. Since the species distribution is that of standard air, the mean free path given by Equation 10 is valid for calculating the Knudsen number. The mean free path is calculated from the Knudsen number and the characteristic length of the body based on the diameter of 0.0127 m. The free stream density is calculated using Equation 10 and the free stream pressure is obtained using the ideal gas law. The free stream pressures required to get the desired Knudsen numbers are given in Table 1. Residuals are continuously monitored for continuity, k, axial-velocity, and radial-velocity. The convergence criterion is that all of these residuals are dropped below 10^{-3} with the mass flow rate and the Mach number of mass-weighted average at throat of inlet retaining constant.

Table 1: Free Stream Parameters for Blunt Body

Knudsen Number	Pressure (Pa)	Mean Free Path (m)	Characteristic Length
0.002	245.59	2.54E-5	0.0127
0.01	49.854	1.27E-4	0.0127
0.05	9.824	6.35E-4	0.0127
0.1	4.912	1.27E-3	0.127

6. RESULTS AND DISCUSSIONS

6.1. Pressure Study

In this study, we observed, as the Mach number increases the pressure also increases, however, an increase in k_n number resulted in decreased density of atmosphere which decreased pressure as well. We noticed that for Mach = 6.5 at Knudsen number 0.1 has the lowest pressure which means too less drag. When it comes to K_n number 0.002 pressure increased parallel drag also increased. Similarly the rest Mach numbers also vary accordingly by change in K_n number.

Pressure obtained for Mach Number=6:5

The change in Mach number hasn't have an effect on Density of the Fluid; so the inputs were given which were calculated for increasing in k_n value. So using this for k_n = 0.002, the pressure generated was around 1117.907KN which is the peak

pressure recorded. Later on, it is decreased by increasing k_n = 0:01; the drag generated was 2274.598KN. It was further diminished to 4480.643KN by increasing the value of k_n = 0:05. Finally for k_n = 0.1, the pressure generate was 2239.041KN, which is too lower compared to all the above.

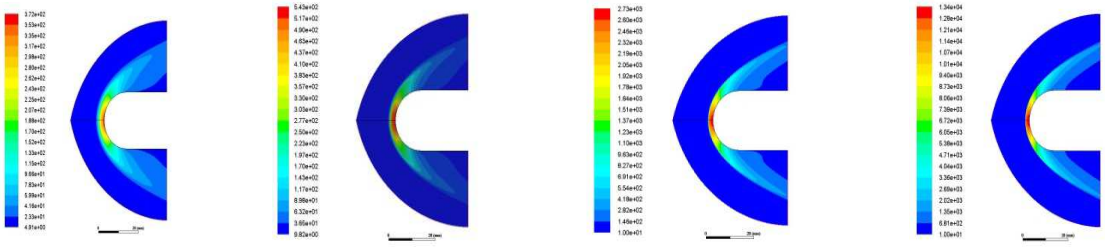

Figure 4: Pressure Variations for Different Knudsen Number for Mach-6.5.

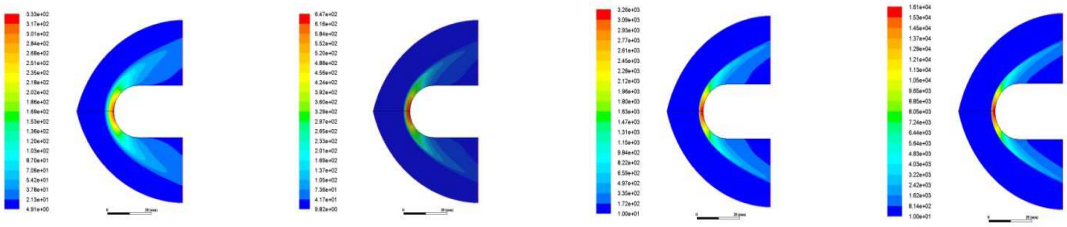

Figure 5: Pressure Variations for Different Knudsen Number for Mach-7.1.

Pressure obtained for Mach number = 7:5

For Mach number M=7.5 and K_n = 0:002, the pressure was recorded around 1588.394KN and it was decreased with the increase of the K_n = 0:01; the pressure generated was 323189:5N. Further, the pressure was diminished to 63664:29N by increasing the K_n = 0:05. Finally, the process was stopped by increasing the K_n = 0:1 which generated pressure of 31817:87N and concluded by less pressure observations.

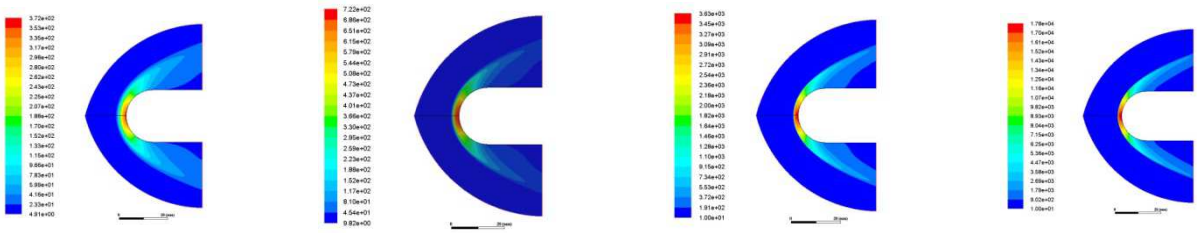

Figure 6: Pressure Variations for Different Knudsen Number for Mach-7.5.

Pressure obtained for Mach number = 8:0

With the increase in pressure generation for each K_n value, there is an effect of increase in Mach number; Where for K_n = 0:002, the pressure generated was about 2411835N and later by increasing the K_n value, the pressure generation was decreased to 490734.6N for K_n = 0:01. Further, pressure was decreased to 96669:16N for K_n = 0:05 which is as low as possible. Even though the pressure generated was low, it further diminished to K_n = 0:1.

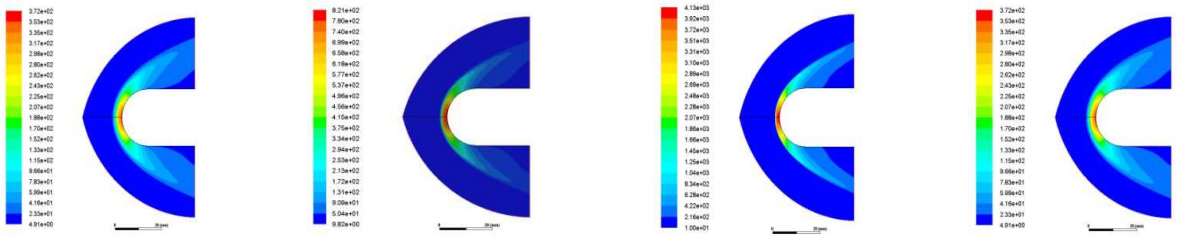

Figure 7: Pressure Variations for Different Knudsen Number for Mach-8.

6.2. Temperature Study

Temperature plots shows decrease in temperature with the increased Knudsen number which results the shock stand-off distance will reduce with the increase in Knudsen number results to decrease in drag during flight. Temperature increased with the increased Mach number. We observed that temperature decreased till M=7.1 and later on temperature rose with an interval of 200K. This shows the heat flux generation on the surface of the vehicle.

Temperature Variation for M = 6:5

During hypersonic speed, the heat flux generation was the major drawback which is generated around 2781.378K for K_n = 0.002, which is the lowest heat flux generated, and later on, it increased to 2810.784K for K_n=0.01. It was observed that the temperature was further increased to 2931.116K and finally concluded with 3931.321K, which the peak temperature is obtained on the blunt body. As the density of the fluid increases, the spacing between molecules increases, which leads to high collaboration of the molecules. This bonding, when a molecule travels and touches to another molecule with high velocity, the temperature increases drastically. Due to this, increase in temperature was recorded for all the K_n numbers.

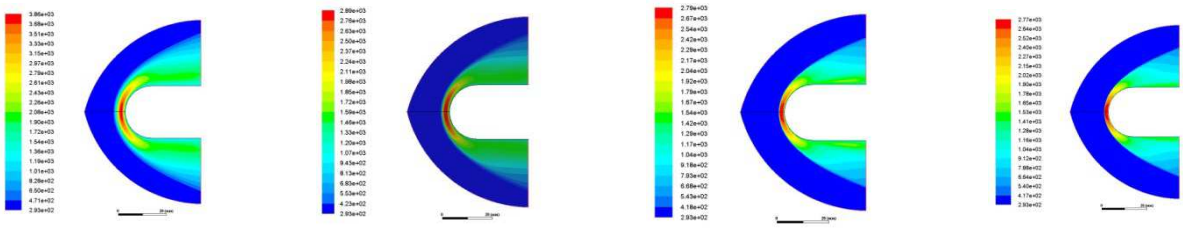

Figure 8: Temperature Variations for Different Knudsen Number for Mach-6.5.

Temperature variation for M = 7.1

As the speed of the vehicle increases, the molecule collaboration also increases and due to loosely packed molecules, the velocity distribution of molecules is higher. This increases the temperature to the peak with the increase in K_n value. We recorded 3260.558K for K_n =0.002 and it increased to 3299.171K by increasing K_n =0.01. The temperature was further increased to 3447.99K for K_n=0.05 and finally ended with peak temperature of 3544.279K.

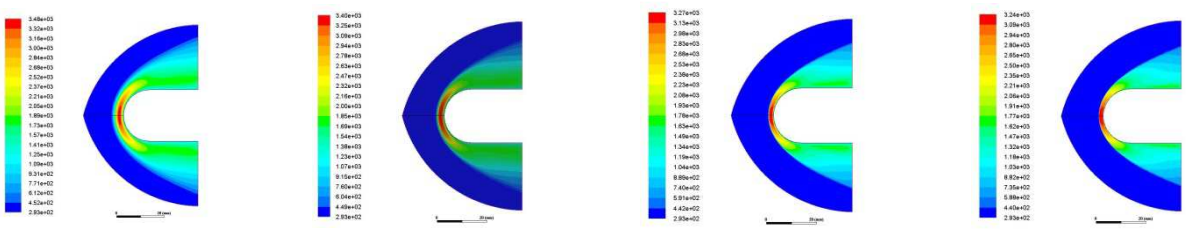

Figure 9: Temperature variations for different Knudsen Number for Mach-7.1.

Temperature variation for M = 7.5

As stated above, temperature increases with an increase in K_n value. For M = 7:5, we observed lowest temperature of 3608:079K for K_n = 0:002 and it elevated slightly by increasing K_n to K_n = 0:01; the temperature obtained was 3647:396;. Later on $K_n$value was increased to K_n = 0:05 also increased the temperature to 3818:46K and finally ended by reaching peak temperature to 3818:46K for K_n = 0:1

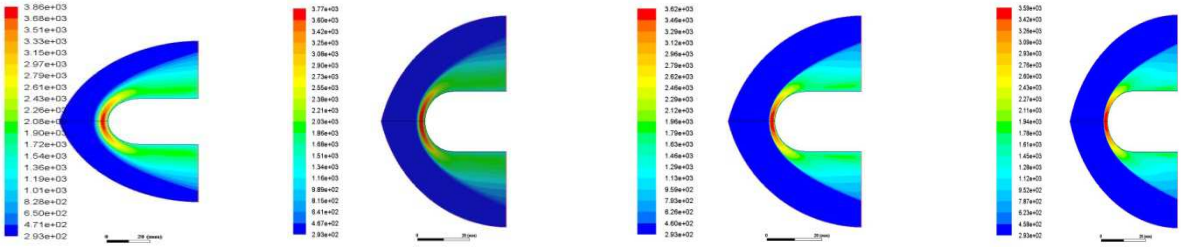

Figure 10: Temperature Variations for Different Knudsen Number for Mach-7.5.

Temperature variation for M = 8:0

Similarly the temperature rises due to velocity increase by the vehicle. It is because of loosely packed molecules, and these molecules collaborate each other with high speed. Our study resulted with a recording of 4311:517N for K_n = 0:002 and it was increased to 4112:455N for K_n = 0:01 and later on it was further increased to 4061:8N by increasing K_n=0.05. Finally, it was concluded by recording peak pressure of for K_n = 0:1.

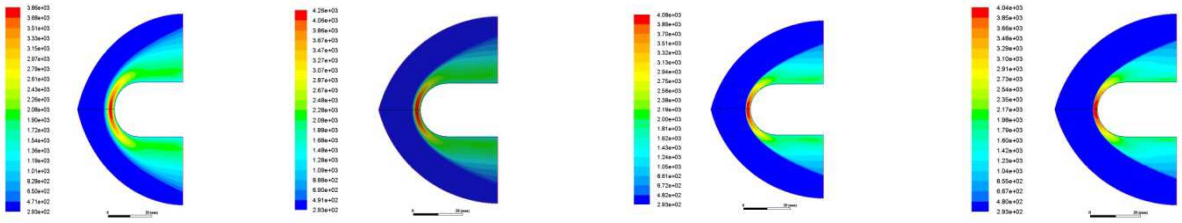

Figure 11: Temperature Variations for Different Knudsen Number for Mach-8.

7. CONCLUSIONS

The study on Drag given in below table gives us decrease in drag with an increase in Knudsen number. But, as the Mach number increases, drag also increases from the table below, it is inferred that there is a drastic reduction of drag for K_n= 0.1, but when it comes to K_n=0.002, we observe only nominal decrease.

Table 2: Drag Estimation for Various Knudsen Number Increasing with an Increased Mach Number

Mach number	K_n=0.002	K_n=0.01	K_n=0.05	K_n=0.1
6.5	1.6108603	0.40040256	0.11345538	2.4E-4
7.1	1.9064469	0.46519763	0.13346742	2.9E-4
7.5	2.1176512	0.51583894	0.14780244	3.3E-4
8	2.3983547	0.58319674	0.16767936	3.7E-4

Pressure plots of various Mach numbers indicate reduction in pressure for increase in Knudsen number and we also observed that drag reduced with an increased Knudsen number. However, pressure increases with an increase in Mach number, but figure 16 shows that pressure ends up at same point for all the Mach numbers.

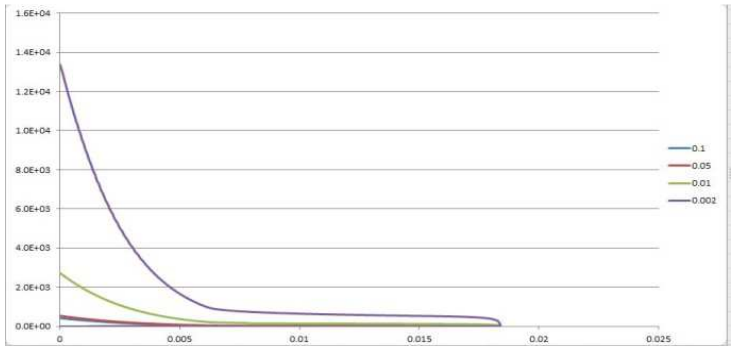

Figure 12: Pressure Plot for M=6.5.

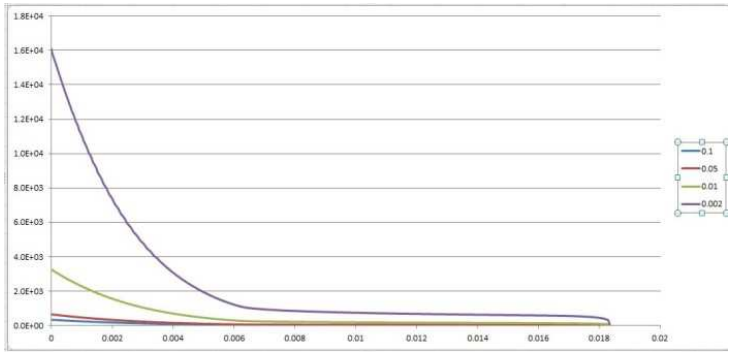

Figure 13: Pressure Plot for M=7.1.

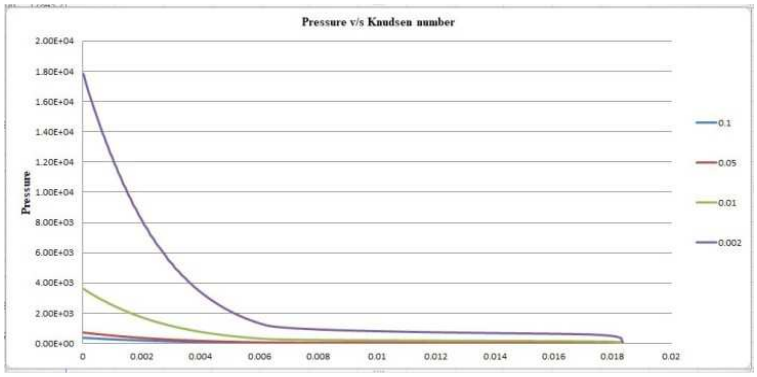

Figure 14: Pressure Plot for M=7.5.

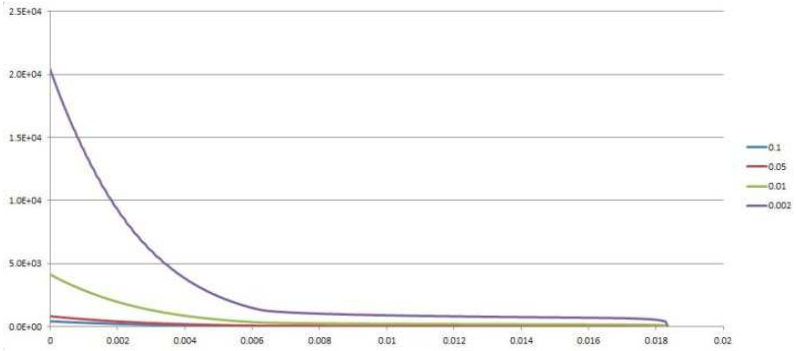

Figure 15: Pressure Plot for M=8 and Negligible.

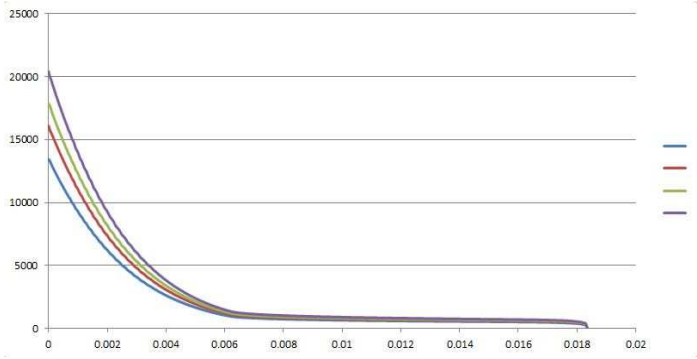

Figure 16: Mach Number vs K_n=245.

In the figure-16, an observation shows that peak drag is generated for low Knudsen number. Hence the drag is reduced with an increase in Knudsen number. Drag of 2:39835N for initial condition of K_n = 245; later on K_n value is increased from 245to K_n = 49:8 which resulted with 0:58319N; further study is performed for K_n = 9:8 which gave 0:16767N. The process was closed after K_n = 4:9 which obtained a drag of 0:00033N which is too small.

REFERENCES

1. *Maxwell J. C. On stresses in rarefied gases arising from inequalities of temperature. Philosophical Transactions of the Royal Society of London, 170:231{256, Jan 1879}.*
2. *Parker J. G. Rotational and Vibrational Relaxation in Diatomic Gases. Physics of Fluids, 2:449{462, 1959}.*
3. *Harvey J. K., Holden M. S., and Candler G. V. Validation of DSMC/Navier-Stokes computations for laminar shock wave/boundary layer interactions part 3. 36th AIAA Thermo physics Conference, AIAA Paper 2003–3643, 2003.*
4. *Kanth, U., Sandeep, C. S., & Prasad, U. S. Comparison of Wall Temperatures on Scramjet Inlets at Hypersonic Velocities.*
5. *Kim K. H., Kim C., and Rho O. H. Methods for the accurate computations of hypersonic flows: I. ausmpw+ scheme. Journal of Computational Physics, 174:38{80, 2001}.*
6. *Holden M. Measurements in laminar regions of shock/shock and shock/bound. Journal of Spacecraft and Rockets, 52:789{803, Feb 2015}.*
7. *Alrobaian, A. A., Khan, S., & Asadullah, M. A New Approach to Low-Cost Open-Typed Subsonic Compressible Flow Wind Tunnel for Academic Purpose.*
8. *Yoon S. and Jameson A. Lower-upper symmetric-gauss-seidel method for the Euler and Navier-stokes equations. AIAA Journal, 26:1025{1026, 1988}.*
9. *Moorthy, C. V., Srinivas, V., Prasad, V. V. S. H., & Vanaja, T. (2017). Computational Analysis of A Cd Nozzle with 'Sed' for A Rocket Air Ejector in Space Applications. 7 (1). Pp 53, 60.*
10. *Zhao W., Chen W., and Agarwal R. Computation of rarefied hypersonic flows using modified form of conventional Burnett equations. Journal of Spacecraft and Rockets, 52:789{803, Feb 2015}.*
11. *Van Leer B. Towards the ultimate conservative difference scheme V: A second-order sequel to Godunov's method. Journal of Computational Physics, 32:101{136, 1979}.*
12. *Khan, S. A., & Mohammed, A. (2018). Passive Control of Base Drag in Compressible Subsonic Flow using Multiple Cavity. IJMPERD, 8, 39–44.*

AUTHOR'S PROFILE

Mr MAMIDI AJAY SAGAR has completed BTech in Aeronautical Engineering and MTech in Aerospace Engineering from MRCET/JNTUH, and currently working as Assistant professor in School of Aeronautics, Neemrana, Rajasthan. His area of interest is High Speed and Experimental Aerodynamics. He had worked in DRDL as a Contract Engineer for one year.

Mr. SYED MUNVAR ALI has completed B.Tech in Aeronautical Engineering and M. Tech Aerospace Engineering from MRCET/JNTUH. Currently working as CFD engineer in DRDL, Hyderabad.

A.NAVYA MANJARI has completed - B.Tech Aeronautical Engineering and presently persuing M. Tech Aerospace Engineering Malla Reddy college of engineering and technology, hyderabad

Ms L. Sushma has completed her B.Tech and M.Tech from JNTUH in Aeronautical Engineering. She has 14 years of experience in teaching and industry. Presently she is persuing PhD in Mechanical Engineering from JNTUH. She has published and presented 7 papers in International Journals, International and National Conferences. She has achieved gold certificate for presenting best paper in ICEMS 2016. Her areas of interest are High speed propulsion and Computational Fluid Dynamics.